



Size-Resolved Stratospheric Aerosol Distributions after Pinatubo Derived from a Coupled Aerosol-Chemistry-Climate Model

Timofei Sukhodolov^{1,2}, Jian-Xiong Sheng³, Aryeh Feinberg², Bei-Ping Luo², Thomas Peter², Laura Revell^{2,4}, Andrea Stenke², Debra K. Weisenstein³, and Eugene Rozanov^{1,2}

¹Physikalisch-Meteorologisches Observatorium Davos and World Radiation Center, Davos, Switzerland.

²School of Engineering and Applied Sciences, Harvard University, MA, United States.

³Institute for Atmospheric and Climate Science, ETH Zurich, Zurich, Switzerland.

⁴Bodeker Scientific, Christchurch, New Zealand

Correspondence to: Timofei Sukhodolov (timofei.sukhodolov@pmodwrc.ch)

Abstract. We evaluate how the coupled aerosol-chemistry-climate model SOCOL-AER represents the influence of the 1991 eruption of Mt. Pinatubo on stratospheric aerosol loading, aerosol microphysical processes, radiative effects, and atmospheric chemistry. The aerosol module includes comprehensive sulfur chemistry and microphysics, in which the particle size distribution is represented by 40 size bins spanning radii from 0.39 nm to 3.2 μm . Radiative forcing is computed online using aerosol optical properties calculated according to Mie theory. SOCOL-AER simulations are compared with satellite and in situ measurements of aerosol parameters, temperature reanalyses, and ozone observations. In addition to the reference model configuration, we performed a series of sensitivity experiments looking at different processes affecting the aerosol layer. An accurate sedimentation scheme is found to be essential to prevent particles diffusing too rapidly to high and low altitudes. The aerosol radiative feedback and the use of a nudged quasi-biennial oscillation help to keep aerosol in the tropics and significantly affect the evolution of the stratospheric aerosol burden, which improves the agreement with observed aerosol mass distributions. Changes in the aerosol distribution affected by an inclusion of Van der Waals forces to the particle coagulation scheme suggest improvements in particle effective radius, although other parameters (such as aerosol longevity) deteriorate. Modification of the Pinatubo emission rate also improves some aerosol parameters, while worsens others compared to observations. Observations themselves are highly uncertain and render it difficult to conclusively judge the necessity of further model reconfiguration. In conclusion, our results show that SOCOL-AER is capable of predicting the most important global-scale atmospheric and climate effects following volcanic eruptions, which is also a prerequisite for improved understanding of anthropogenic effects from sulfur emissions.

1 Introduction

During the eruption of Mt. Pinatubo in June 1991, a large amount of sulfur dioxide was emitted into the stratosphere, leading to an enhancement of the stratospheric aerosol burden. The aerosol layer perturbed the Earth's radiative balance, resulting in a top-of-the-atmosphere global mean radiative forcing of approximately -3 W m^{-2} (Minnis et al., 1993), a global surface cooling of $\sim 0.4\text{-}0.5 \text{ K}$ (Dutton and Christy, 1992; Thompson et al., 2009), and a temperature increase of $\sim 2.5\text{-}3.5 \text{ K}$ in the tropical



lower stratosphere (Labitzke and McCormick, 1992; Randel et al., 2009). During the past decades it was shown that these observed temperature perturbations are connected to many feedbacks in the Earth system such as alteration of the stratospheric circulation with consequences for the troposphere (e.g., Kodera, 1994; Graf et al., 2007), dynamical and chemical effects on stratospheric ozone (Solomon, 1999; Rozanov et al., 2002; Telford et al., 2009), drying of the troposphere causing significant changes in the regional hydrological cycle (Soden et al., 2002), modulation of the global monsoon (Liu et al., 2016), and even modulation of the ocean circulation (e.g., Predybaylo et al., 2017). The distribution and evolution of the stratospheric sulfate can, therefore, be considered as the main forcing for these and many other processes following large volcanic eruptions (Kremser et al., 2016; Timmreck et al., 2016; Swingedouw et al., 2017) and proper information about the aerosol layer is crucial for the characterization and understanding of numerous inherent feedbacks.

Modeling studies help to synthesize our knowledge of how the Mt. Pinatubo and other big eruptions impact the climate system. As a first approximation, global three-dimensional general circulation models (GCMs) or chemistry-climate models (CCMs) used for studying the volcanic effects on climate can be discretized into two groups: those using prescribed aerosol distributions and those using online aerosol microphysical modules (e.g., Zanchettin et al., 2016). Models of the first type use aerosol composites derived from satellite and ground-based observations, but for studies of the pre-satellite era and the future such models have to rely on estimates provided by models of the second type. Therefore, they have only limited ability to address climate feedbacks, as the aerosols are prescribed, and also either inherit instrumental uncertainties (see Section 3) or uncertainties inherited from the second type of models. Models with aerosol microphysics can also be grouped, depending on how they treat the aerosol size distribution: a first class of so-called “modal” and “bulk” (unimodal) schemes and a second class of size-bin resolving (also called “sectional”) aerosol modules. Currently, there are more than a dozen active global models with aerosol microphysics (see review by Kremser et al., 2016), a smaller part of which employ sectional aerosol schemes.

Size-dependent aerosol sedimentation rates crucially affect the stratospheric aerosol lifetime. Arfeuille et al. (2013) argued that bulk schemes are less satisfactory in reproducing volcanic aerosol size distributions, which cast doubts on the success of such approaches. For 2D models, Weisenstein et al. (2007) have shown that size-bin resolving aerosol models are superior to modal approaches in accurately representing the time-dependent aerosol size distribution after large volcanic eruptions. Further progress using a CCM coupled with a size-bin resolving microphysical aerosol module to simulate Pinatubo-like eruptions has been achieved by English et al. (2013), however the decline of the simulated aerosol burden was too fast compared with observations, which they attributed to the lack of heating as the aerosol radiative feedback remained decoupled in their model. This highlighted that the fine resolution of aerosol sizes is not a universal problem solution and performance of any model, even with highly resolved aerosol sizes, depends on representation of relevant chemical, microphysical and radiative processes, large-scale transport and gravitational sedimentation, as well as their interactions.

The Pinatubo eruption is the strongest volcanic event since the beginning of the satellite era and therefore often used as a model performance test. Modeling studies of the Pinatubo eruption using models with an assumed log-normal size distributions (e.g., Timmreck et al., 1999a, b; Aquila et al., 2012; Dhomse et al., 2014; Sekiya et al., 2016; Mills et al., 2016) and sectional distribution (English et al., 2013; Kleinschmitt et al., 2017) generally agree reasonably well with observations of atmospheric long-wave and short-wave extinctions, aerosol burden, and other integral parameters. However, an intercomparison of different



Pinatubo studies is hampered by the fact that models make different assumptions of how much sulfur was initially emitted and how the plume was distributed as function of altitude. Models that reported good agreement with observations used a variety of emission estimates ranging from 10 to 17 teragrams (Tg) of SO_2 and SO_2 plume altitudes in the lower stratosphere differing by a few kilometers. This hints at large uncertainties of how models treat important microphysical and transport processes.

- 5 A recent Model Intercomparison Project on the climatic response to Volcanic forcing (VOLMIP, Zanchettin et al., 2016) aims to address the existing intermodel uncertainties. However, so far only the Tambora eruption in 1815 has been considered for the global models with interactive aerosol microphysics. Marshall et al. (2017) evaluated the performance of four state-of-the-art models (WACCM, UM-UKCA, SOCOL-AER, and ECHAM5-HAM) using mostly the same settings of the initial emission and compared the results to the available observations of ice-core sulfate. The focus of that study was on sulfate
- 10 deposition in polar areas, as ice cores are the best available source of information about historical eruptions (Sigl et al., 2015; Toohey and Sigl, 2017). The comparison revealed that modelled volcanic sulfate deposition varies substantially in timing, spatial pattern and magnitude between the models. The ratio of the hemispheric atmospheric sulfate aerosol burden after the eruption to the average amount of sulfate deposited on ice sheets varied among models by up to a factor of 15. The burden-to-deposition ratio is to a large extent determined by the treatment of deposition processes, which are simplified in models.
- 15 Furthermore, it also depends on sulfur species, which never entered the stratosphere but were transported through the (upper) troposphere, oxidized and removed by wet or dry deposition. Moreover, it depends on how fast aerosols grow and sediment from the stratosphere back to the troposphere. The analysis of the stratospheric burdens of SO_2 and liquid H_2SO_4 as well as the polar winds, also revealed large intermodel differences. Therefore there is still no clear understanding of which model is closer to reality in describing the stratospheric aerosol distribution, since direct stratospheric observations are missing and the
- 20 ice core estimates could be strongly modulated by the tropospheric deposition schemes.

Table 1. List of Experiments

Name	QBO nudged	Aerosol feedback	Sedimentation scheme	Coagulation Efficiency α	Emission rate [Tg SO_2]
REF	Yes	Yes	Walcek	$\alpha = 1$ everywhere	14
REF12	Yes	Yes	Walcek	$\alpha = 1$ everywhere	12
UPWIND	Yes	Yes	Upwind	$\alpha = 1$ everywhere	14
RAD	Yes	No	Walcek	$\alpha = 1$ everywhere	14
QBO	No	Yes	Walcek	$\alpha = 1$ everywhere	14
RADQBO	No	No	Walcek	$\alpha = 1$ everywhere	14
COAG	Yes	Yes	Walcek	α based on a Lennard-Jones potential: $\alpha \sim 1$ in continuum regime ($K_n \gg 1$); $\alpha \sim 1-3$ in transition regime ($K_n \sim 1-10$); $\alpha \ll 1$ in free molecular regime ($K_n \ll 1$).	14



The representation of aerosol evolution in the stratosphere requires treatment of many processes, which can substantially differ among models. Previous studies (e.g., Timmreck et al., 1999a, b; Aquila et al., 2012) illustrated the importance of the quasi-biennial oscillation (QBO) and radiative heating of volcanic aerosols in the models, as these processes affect the transport and thus the lifetime and climate impact of aerosols. Benduhn and Lawrence (2013) found that numerical diffusion induced by an inaccurate sedimentation scheme may lead to excessive transport of the aerosol to the middle and upper stratosphere. So, even with a fine aerosol size resolution, resulting sedimentation can be biased due to the model's numerical scheme. English et al. (2011, 2013) suggested that attractive van der Waals forces may lead to an enhanced coagulation efficiency and should be taken into account (in the transition and free molecular regimes). However, such interactions led to an even faster decay in their simulated global aerosol burden after the Pinatubo eruption. Sekiya et al. (2016) and Kleinschmitt et al. (2017) also investigated the role of this process and reported significant effects on aerosol parameters. Interactive chemistry was also shown to be important for aerosol formation, as hydroxyl radical (OH) can become depleted after big eruptions, which prolongs the time needed for conversion of volcanic SO₂ to H₂SO₄ (Bekki, 1995; Mills et al., 2017).

The coupled size-resolving stratospheric aerosol-chemistry-climate SOCOL-AER model has been evaluated in detail for volcanically quiescent conditions (Sheng et al., 2015b). In this study, we employ it for the Pinatubo eruption of 1991 and aim to characterize its performance comparing our results against satellite observations and in-situ measurements. By means of this model we also attempt to illustrate the roles of the aerosol radiative heating, sedimentation scheme, coagulation efficiency, and quasi-biennial oscillation (QBO) in the evolution of the aerosol burdens, aerosol optical properties and particle size distributions, which may also help to better understand differences between various models.

2 Method

The coupled aerosol-chemistry-climate model SOCOL-AER has been introduced by Sheng et al. (2015b), who applied the model to analyze the global atmospheric sulfur budget under volcanically quiescent conditions and its sensitivity to anthropogenic emissions. SOCOL-AER includes a comprehensive description of sulfur chemistry and microphysics, in which the particles are size-resolved by 40 size bins spanning radii from 0.39 nm to 3.2 μm. Interactive aerosol radiative feedback at all wavelengths is also taken into account. The aerosol optical properties required by the radiation code are calculated online from aerosol physical properties using Mie theory. In this study, the spatial resolution of SOCOL-AER is set to T42 horizontal truncation (2.8° × 2.8° latitude/longitude resolution) and 39 vertical hybrid sigma-pressure levels from the surface to 80 km (about 1-1.5 km per level in the upper troposphere and lower stratosphere, 2-3 km above). The QBO in the model is nudged to observed wind profiles. Monthly mean sea surface temperatures (SSTs) and sea ice coverage (SIC) are prescribed. Comprehensive sulfur surface emissions are also fully taken into account.

The 1991 Pinatubo eruption is introduced by an injection of 14 Tg SO₂ in the region 97°-112°E and 1.8°S-12°N according to observations (Guo et al., 2004). SO₂ is released continuously from 14 to 15 June 1991 and spread between 16 to 30 km with a vertical mass distribution optimized according to Sheng et al. (2015a), skewed to low altitudes with the mass peak between 18 and 21 km. This establishes a realistic initial mass loading of the eruption. All experiments are summarized in Table 1. The



reference run subsequently termed REF represents the standard setup of SOCOL-AER, including nudged QBO, interactive aerosol radiative feedback, and coagulation efficiency uniformly set to one. In terms of module versions it replicates the model configuration used for the Tambora study (Marshall et al., 2017).

By means of the experiment REF12 we estimate the model sensitivity to uncertainty in emission amount by lowering it to 12 Tg SO₂. In the experiment termed RAD, the radiative fluxes are calculated using the SAGE-4λ dataset (Arfeuille et al., 2013) averaged over the period 1995-2002 instead of the interactively simulated aerosol distribution, which eliminates the radiative effects of volcanic aerosols. The experiment termed QBO is carried out without QBO, which leads to a weak easterly zonal wind in the tropical stratosphere. Both QBO nudging and interactive radiation are switched off in the experiment termed RADQBO. These three experiments allow us to identify the impact of QBO and radiative heating of volcanic aerosols on the evolution of the stratospheric aerosol burden after Pinatubo. We also consider two exploratory experiments concerning the coagulation efficiency. The experiment termed COAG represents the coagulation efficiency as Lennard-Jones potential, i.e. a smooth function of the Knudsen number retrieved from the results in Figure 3 of Narsimhan and Ruckenstein (1985) with a Hamaker constant of 5×10^{-19} J. As an approximation of attractive Van der Waals forces it enhances the coagulation efficiency in the transition regime (maximum enhancement larger than 2), but decreases it rapidly (less than 1) as the Knudsen number increases in the free molecular regime. The experiment termed UPWIND employs the upwind sedimentation scheme (Benduhn and Lawrence, 2013), while all other simulations use the more elaborate Walcek method with minimal numerical diffusion (Walcek, 2000). This is sufficient to clarify the impact of different sedimentation schemes, though work by Benduhn and Lawrence (2013) presented a further improved modified Walcek method.

For each of these experiments we calculated five ensemble members. In the figures we show ensemble spread for the REF experiment and only ensemble means for other experiments to keep figures as uncomplicated as possible. In addition to Pinatubo, for all runs we considered the smaller eruption of Cerrro Hudson in Chile in August 1991. We used the latest estimate of 2.3 Tg total SO₂ emitted (Miles et al., 2017). Sensitivity studies with and without this event showed that its contribution is minor, since it is located at higher latitudes (45.5°S), but we keep it for completeness.

3 Results and discussion

3.1 Aerosol Burden

Figure 1 shows the evolution of observation-derived and model-calculated stratospheric aerosol burdens in units of teragram (Tg) of sulfur globally integrated (a) and in the tropics (b). The High-Resolution Infrared Radiation Sounder (HIRS) measured the aerosol vertical column and derived total aerosol mass with about 10% uncertainties. HIRS includes tropospheric and stratospheric aerosols together (Baran and Foot, 1994). In contrast, the limb-occultation measurements of SAGE II allow aerosols in the troposphere and stratosphere to be distinguished from one another. In this work the SAGE II-derived total aerosol mass is represented by two data sets. The first one, the SAGE-4λ method (Arfeuille et al., 2013), used within the Chemistry-Climate Model Initiative (CCMI), employs all four SAGE wavelengths with overall about 30% uncertainties for non-gap-filled data and higher uncertainties in data gaps filled by lidar station data. The second data set was recently compiled

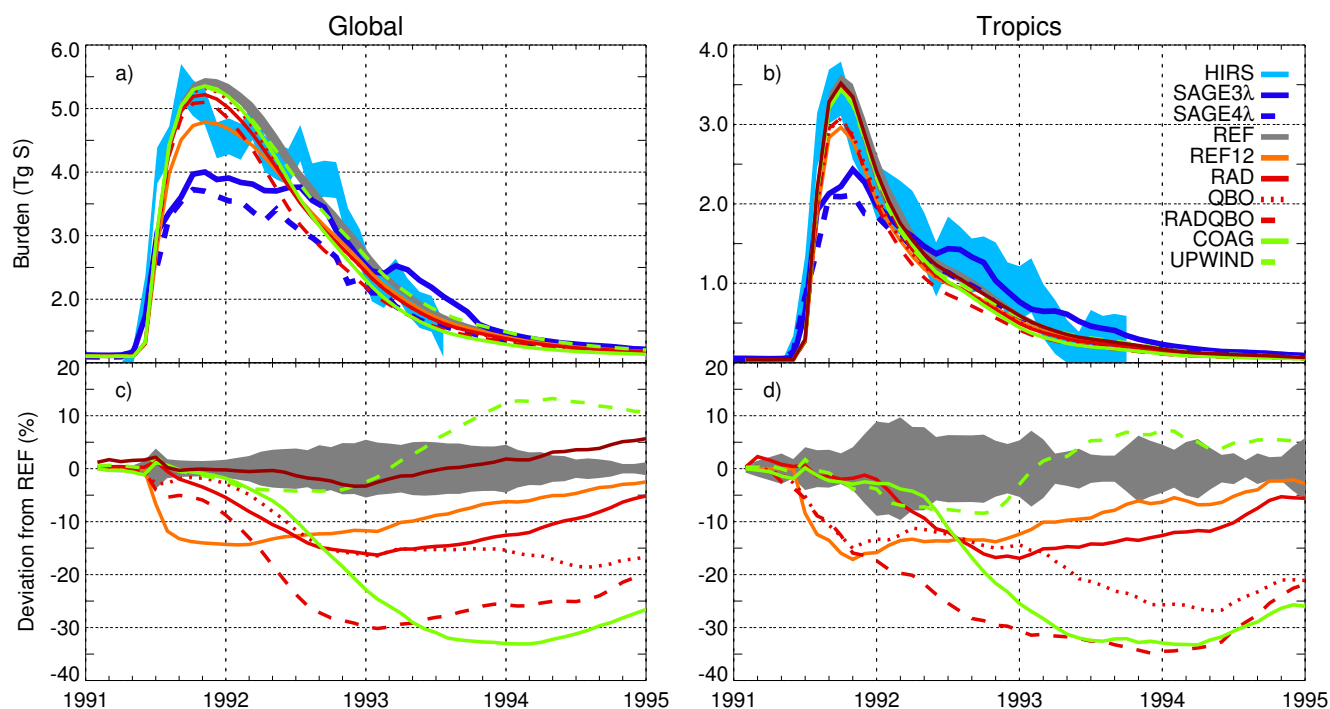


Figure 1. Panels a and b: evolution of model-calculated global (pole to pole, left) and tropical (20°S—20°N, right) stratospheric aerosol burden (Tg of S) compared with the HIRS and SAGE II-derived data (SAGE-3,4λ). HIRS-derived aerosol sulfur burden assumes 75% sulfuric acid by weight. Light blue shaded area: uncertainties of HIRS. Grey shaded area: 2-σ ensemble spread of the REF experiment. All other experiments are shown as ensemble means. Panels c and d: same as a and b, but deviations of all the numerical experiments from the REF in %.

for phase 6 of the Coupled Model Intercomparison Project (CMIP6, Eyring et al., 2016) using the SAGE-3λ method, which is similar to SAGE-4λ but refrains from employing the less reliable channel at 385 nm, thus considering only three SAGE wavelengths. Directly after Pinatubo the SAGE-3λ data set uses additional satellite and ground-based data for gap-filling. More information about the SAGE-3,4λ composites can be found in a recent paper by Revell et al. (2017).

- 5 During the first year after Pinatubo, the aerosol mass in both SAGE II-based data sets is noticeably lower than HIRS. This is likely related to the saturation effects of SAGE II, as a limb-occultation instrument, during this period (Russell et al., 1996). The SAGE-3λ composite provides significantly larger burdens than its predecessor, due to additional data used in a gap-filling procedure (Revell et al., 2017), but still much lower than HIRS. After this period, when the atmosphere becomes sufficiently transparent, SAGE II measurements are expected to provide more accurate aerosol extinctions. In contrast, the HIRS-derived
- 10 mass becomes less reliable with time, when the aerosol cloud spreads to higher latitudes with lower values that are close to the noise level of the technique (Baran and Foot, 1994). This suggests to trust the HIRS data up to mid-1992 and the SAGE data afterwards (Sheng et al., 2015a). Note, however, that the updated SAGE II-based data set now also provides values closer to HIRS from mid-1992 to early 1993 and considerably larger values later in 1993.



The global stratospheric aerosol burden calculated by REF (grey shaded area representing $2\text{-}\sigma$ ensemble spread) agrees well with the HIRS data peaking around 5.4 Tg at the end of 1991. Later, REF agrees well with the SAGE-4 λ composite, while the updated SAGE-3 λ has a generally larger burden. Qualitatively similar results are found for the tropics. Recent modelling studies by Mills et al. (2016) and Kleinschmitt et al. (2017) showed very similar time series of the global aerosol burden with initial emissions of 10 and 14 Tg of SO₂, respectively. These studies, another work by Sekiya et al. (2016), as well as the present study fail to reproduce the pronounced step-like evolution of the burden seen in HIRS and SAGE-3 λ , showing a smoother decrease instead. Dhomse et al. (2014) overestimated the HIRS peak burden even with 10 Tg of SO₂ emitted, but obtained this step-like behavior. Dhomse et al. (2014) explained it by variability of the background aerosols related to the summer increase of photolysis, but they also noted that their background values are significantly larger than in the other models and observations. Besides instrumental uncertainty, another reason for the complicated shape of the observational curves seen in Fig. 1 could be the seasonal variability of the stratospheric circulation that is known to be underestimated in ECHAM5 (Stenke et al., 2013) and LMDZ (Kleinschmitt et al., 2017), which are core GCMs of the sectional models SOCOL-AER and LMDZ-S3A, respectively.

Panels c and d of Figure 1 show deviations (%) from REF of all experiments. Our experiment with lower emission (REF12, 12 Tg of SO₂ instead of 14 in REF, but otherwise unchanged plume characteristics) shows lower burdens of up to 14% globally and 17% in the tropics, which is therefore even farther than REF from the latest SAGE II-derived estimates after mid 1992. The results of the sensitivity runs QBO, RAD and RADQBO are presented by the red curves. During the first few months after the Pinatubo eruption, the aerosol mass loading in the tropical reservoir is maintained by the balance between sedimentation and enhanced tropical upwelling due to radiative heating of the volcanic aerosols with the QBO in a strongly descending easterly phase (Trepte and Hitchman, 1992; Trepte et al., 1993). Therefore, deactivation of each of these processes leads to a stratospheric burden decrease mostly located in the tropics. About one year after the eruption the global aerosol burden in QBO and RAD is approximately 15% lower than in REF. The experiment RADQBO shows a cumulative effect up to -30% around 1993. Gravitational sedimentation becomes a dominant removal process when particles grow sufficiently large after the Pinatubo eruption. With effective radii of 0.5 μm or more (Russell et al., 1996) these particles sediment efficiently. The burden calculated by UPWIND mostly lies within $\pm 10\%$ with respect to REF. This upwind scheme was shown to have a large numerical diffusion smearing the aerosol layer out in both, up and down, directions (Benduhn and Lawrence, 2013). This results in a slightly lower mass during 1-1.5 years after the eruption (effect of the downward diffusion), and a slightly larger mass later on (upward transported aerosols stay longer in the stratosphere). Although this diffusion effect is of numerical origin, for our model it increases the stratospheric lifetime of aerosols and leads to a better agreement with SAGE-3 λ after 1993. The aerosol burden calculated by COAG, which differs from REF by a higher coagulation efficiency, shows a more rapid decay rate of the global volcanic aerosol burden compared to REF and the measurements. The difference to REF maximizes in late 1993 at approximately -33%, which is in agreement with other studies also looking at the van der Waals forces effects (English et al., 2013; Sekiya et al., 2016).

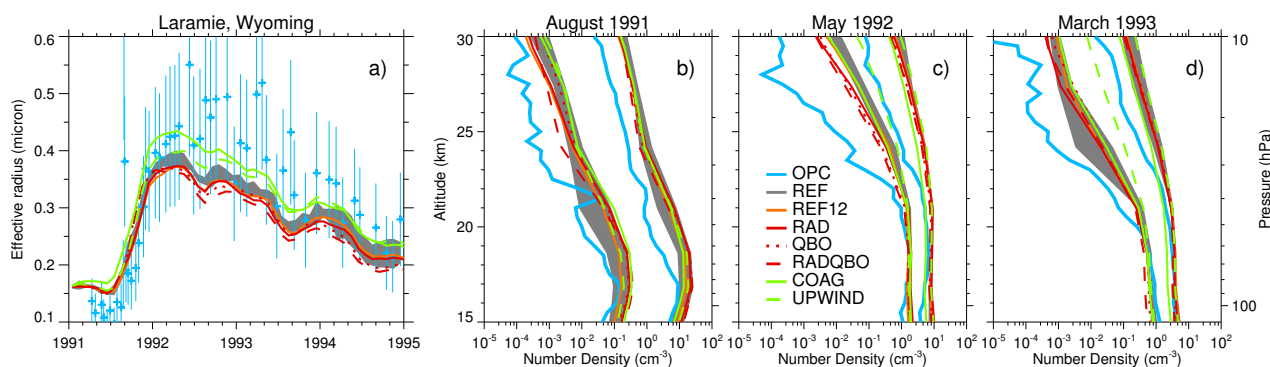


Figure 2. Comparison of in situ measurements of particle size (at Laramie, Wyoming, Deshler (2008)) with SOCOL-AER simulations. (a) Stratospheric effective particle radius averaged for 14–30 km altitude. Thin blue whiskers reflect measurement uncertainty (taken from Kleinschmitt et al. (2017)). (b–d) Profiles of cumulative number densities for two size channels with radii $R > 0.15 \mu\text{m}$ (right group of curves) and $R > 0.5 \mu\text{m}$ (left group of curves) in August 1991, May 1992, and March 1993, respectively.

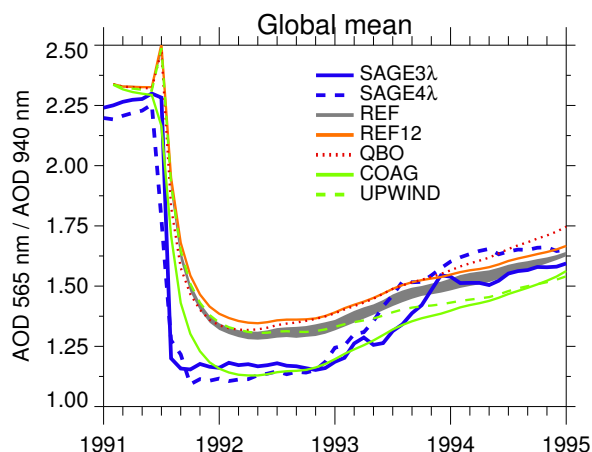


Figure 3. Comparison of remote measurements of aerosol optical depth (AOD) ratios at two wavelengths, a proxy of particle size, with SOCOL-AER simulations. Lines: SAGE II-derived (SAGE-3,4 λ) and modeled global AOD (> 18 km) ratios 565 nm / 940 nm. Grey shaded area: 2- σ ensemble spread of the REF experiment. All other experiments are shown as ensemble means.

3.1.1 Aerosol size distribution

Figure 2 shows comparisons of the optical particle counter (OPC) measurements operated above Laramie, Wyoming (41°N, 105° W, Deshler et al., 2003; Deshler, 2008) against our model experiments. Panel a shows the effective aerosol radius averaged over 14–30 km. The effective radius calculated by REF generally lies within the observational uncertainty. However, compared to the observational mean, it is biased high under quiescent conditions and biased low during the volcanically perturbed period. COAG shifts the effective radius up compared to REF which improves the agreement with observations after 1992, but worsens



it earlier. Differences of other experiments reflect the burden of the aerosol behavior shown in Fig. 1, illustrating that less mass present in the stratosphere generally also leads to smaller sizes.

Panels b-c of Fig. 2 show cumulative number distributions for two OPC size channels ($R > 0.15 \mu\text{m}$ and $R > 0.5 \mu\text{m}$) in August 1991, May 1992, and March 1993 representing different stages of the volcanic aerosol cloud. We use months with at least two soundings to obtain a useful approximation of monthly means. Aerosol number densities at the altitudes of the maximum concentrations is well reproduced by REF for both large and small particles. Higher altitudes, however, are less well reproduced, with modeled number densities being up to one order of magnitude too high at certain levels. However, at these high altitudes OPC measurements are themselves uncertain, often having to rely on only one or two channels (plus the concomitant condensation counter measurement). Very large deviations from the OPC measurements by up to two orders of magnitude are found for the UPWIND experiment, which has clearly too many particles, especially large ones, in the middle stratosphere all the way to the upper edge of the stratospheric aerosol layer, highlighting the importance of a sedimentation scheme with low numerical diffusivity. Experiments with radiatively decoupled aerosols, RAD and RADQBO, illustrate the importance of the enhanced upwelling, even in midlatitudes, by showing more large particles staying at the lower levels.

To analyze the globally mean size distributions, in Fig. 3 we show the ratio of aerosol optical depths (AOD) at 565 nm and 940 nm for the column above 18 km, calculated from SAGE II-derived composites (blue curves) and from model results. These ratios are inversely related to the particle size: a smaller ratio corresponds to larger particles. In the early phase of the Pinatubo eruption, a large number of small particles are formed, which coalesce very quickly as shown by the very sharp drop in the AOD ratio, falling below 1.25 in observations. Afterwards, the small AOD ratio stays almost constant for approximately one year. Around late 1993 the ratio starts to return to higher values, because the large particles continuously sediment out of the stratosphere and smaller particles nucleate in the air entering the stratosphere in the tropics. REF predicts smaller particles than derived from SAGE II during the early phase after the eruption, and only in 1993 it begins to agree well with the satellite observations. In contrast, due to the enhanced coagulation, COAG produces larger particles (smaller AOD ratios) than REF, and shows better agreement with SAGE II during the four years following the eruption. The model run UPWIND with a simplified upwind scheme for sedimentation is initially close to REF but starts to overestimate the particle sizes compared to REF after 1993. This is related to a larger aerosol burden (Fig. 1), which enables further coagulation. Our experiment with the reduced emission (REF12) further illustrates this effect by showing that weaker emission leads to slightly smaller sizes over the whole lifetime of the volcanic aerosol cloud.

In general, all model experiments show the same global and local effects compared to each other and to the two observational datasets, in-situ OPC measurements and the satellite-based global composites SAGE-3 λ and SAGE4 λ . The main difference is seen during the pre-eruption time, as the model shows larger particles than OPC and smaller particles than SAGE, which can be attributed to the local bias of model parameters.

3.2 Aerosol optical depth

Figure 4 shows the latitudinal evolution of volcanic material as modelled and measured AOD in the visible part of the solar spectrum, which also represents the main direct climate forcing, since it defines the amount of scattered solar irradiance

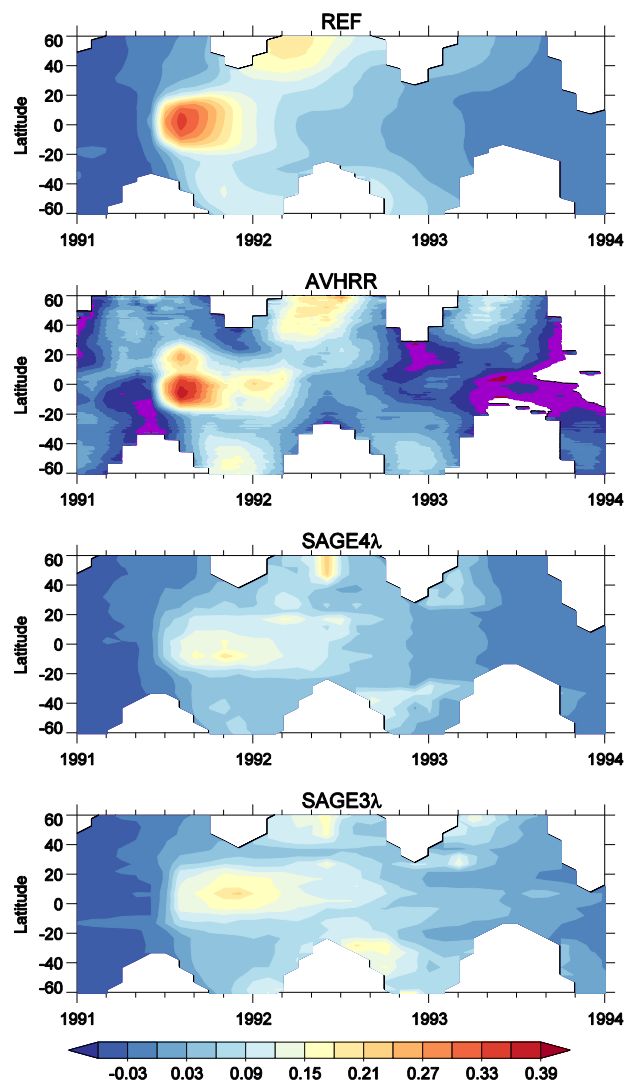


Figure 4. Monthly zonal average total AOD over oceans measured at $0.63 \mu\text{m}$ by AVHRR and calculated at $0.56 \mu\text{m}$ by SOCOL-AER and provided by SAGE3,4 λ composites. Background values are subtracted from all data sets (which may result in slightly negative values). All panels are masked at winter high latitudes where AVHRR data are missing.

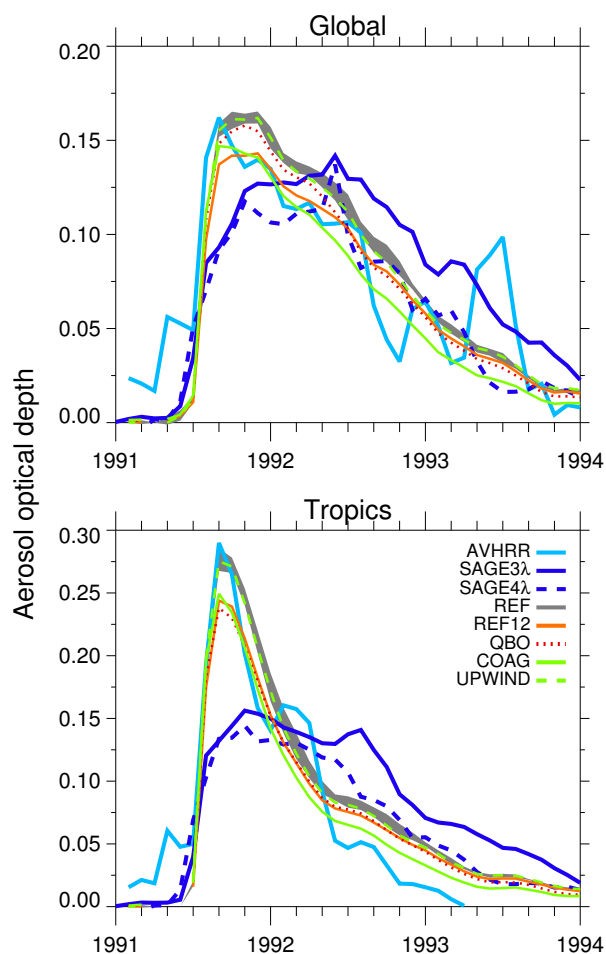


Figure 5. Same as in Fig. 4 but averaged globally (80°S - 80°N) and in the tropics (20°S - 20°N). Grey shaded area: $2\text{-}\sigma$ ensemble spread of the REF experiment. All other experiments are shown as ensemble means.

responsible for global cooling. In addition to SAGE II, we used data from the Advanced Very High Resolution Radiometer (AVHRR) satellite instrument, which makes observations over global oceans (Zhao et al., 2013). Modeled and SAGE-3,4 λ AODs are obtained by vertically integrating the extinctions. We removed latitudes not observed by AVHRR for each month from the other data sets and subtracted background values from observations and calculations, thereby excluding also the contributions from tropospheric aerosols. Aerosol optical depths derived from SAGE II and AVHRR significantly disagree with each other both in magnitude and spatial distribution. SAGE-3,4 λ show much smaller AOD in the tropics in 1991 and do also not show a strong southward plume as seen in AVHRR at the end of 1991, part of which is influenced by the high-latitude Cerro Hudson eruption in August 1991. The northern hemispheric plume in 1992 is also more pronounced in the AVHRR data. Figure 5 shows the same AOD values, but averaged over the globe and the tropics. The main difference between AVHRR and



SAGE is that AVHRR shows a higher AOD peak in 1991 (two times higher in tropics), similar to the faster increase in early aerosol burden of HIRS (Fig. 1). However, AVHRR reveals a much faster decay, so that starting from 1992 SAGE II-derived AOD is much larger than measured by AVHRR.

Modeling results are overall closer to AVHRR than to SAGE II-derived data. REF shows weaker south- and northward
5 plumes in Fig. 4, but perfectly captures the initial increase in the tropics seen by AVHRR. The lifetime of the initial tropical cloud is also well captured compared to AVHRR, except for a small increase in early 1992, while in both SAGE II-based data sets the cloud persists for much longer. Similarly to the burden shown in Fig. 1, starting from mid-1992 the model results are closer to SAGE-4 λ than to SAGE-3 λ . The experiment REF12 shows lower AODs that are, however, even closer to AVHRR. The experiment without QBO shows that less mass is maintained in the tropics compared to REF, and therefore more mass is
10 transported southward in 1991 following the Brewer-Dobson circulation. The experiment with increased coagulation efficiency (COAG) shows faster decay of initial AOD increase, while in UPWIND it is the opposite. Similarly to the size evolution discussed in the previous section, in general, details of all modeling experiments are also qualitatively consistent to those shown for the the burden in Fig. 1.

3.3 Stratospheric temperature response

15 Lower tropical stratospheric warming after major eruptions is one of the key features of volcanic influence on climate (e.g. Swingedouw et al., 2017). Besides being a forcing for the thermal wind balance, a mechanism through which volcanoes can affect high latitude tropospheric circulation, this warming is also an important indicator for aerosol mass distribution in the stratosphere. Infrared absorption of volcanic aerosols does not critically depend on aerosol particle size, but the radiative warming is directly related to the total aerosol mass density (Lacis et al., 1992). The difficulty of correct representation of
20 post-volcanic stratospheric warmings is a known issue of global models. Key factors are, besides uncertainties in aerosol distributions, model dynamics and radiative transfer, which in turn also depends on many factors such as spatial and spectral resolution, presence and quality of interactive chemistry and others (Eyring et al., 2006; Lanzante and Free, 2008; CCMVal, 2010).

Figure 6 compares zonal-mean tropical temperature anomalies computed by SOCOL-AER in the lower stratosphere after
25 the Pinatubo eruption with ERA-interim and MERRA reanalyses. Anomalies are calculated by subtracting the climatological annual cycle and the QBO impact. Since the lower tropical stratosphere is a dynamically very active region, the model also shows a large ensemble spread in the stratospheric temperature signal so that all numerical experiments and observations generally fall into this variability. While the temperature anomalies in the reanalyses differ by up to 1 K, the ensemble mean of REF (black curve) overestimates the warming both at 30 and 70 hPa by 1-2 K in late 1991 and mid-1992. The SOCOL-AER
30 scenarios show some differences with respect to each other. While the experiment with the reduced emission (REF12) shows better agreement with reanalyses at both levels, this apparent improvement comes with clear deteriorations in other quantities, such as too small particle sizes (Fig. 3). The scenario with enhanced coagulation efficiency COAG is warmer at 70 hPa early in 1992, which is related to increased sedimentation of larger particles to lower altitudes. Results of the UPWIND scenario show

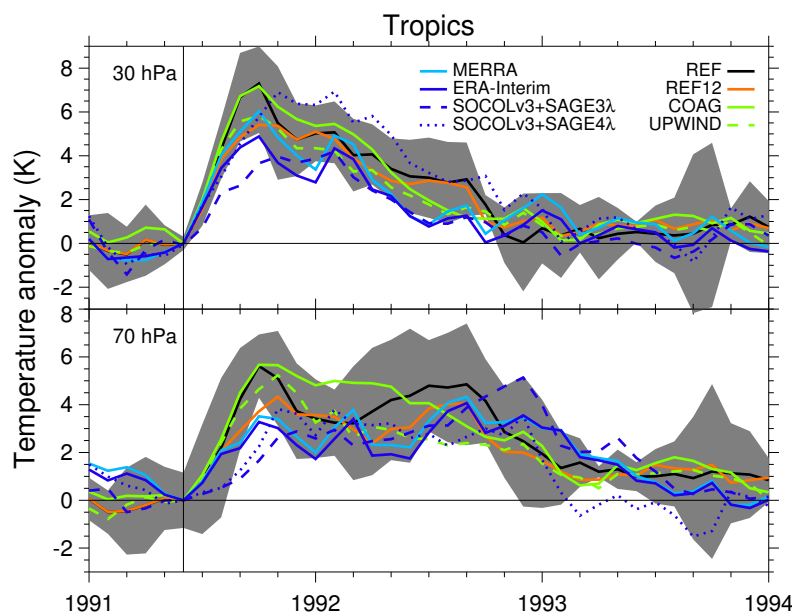


Figure 6. Zonal mean temperature anomalies from SOCOL-AER for tropics (20°S – 20°N) at 30 hPa (top) and 70 hPa (bottom). Light and dark blue lines: MERRA and ERA-Interim temperature reanalysis data. Anomalies are computed by subtracting the annual cycle and QBO. Grey shaded area: $2\text{-}\sigma$ ensemble spread of the REF experiment. All other scenario curves are ensemble means.

a smaller warming than REF, which reflects the larger vertical spread of the aerosol mass due to enhanced diffusion leading to faster aerosol removal from the lowermost stratosphere.

To further understand the model results, we plotted the vertical aerosol mass distribution in the tropics for REF and the SAGE-3,4 λ composites in Fig. 7. We did not plot the vertical mass distributions from other experiments because they are all very similar to REF relative to SAGE data. There are small differences between experiments that are consistent with the previous analysis, i.e. the UPWIND mass is more vertically diffused, while COAG results show faster decay of the whole aerosol cloud and therefore slightly more mass present at lower levels. The main difference of all model experiments to SAGE II-derived data and especially to the latest SAGE-3 λ composite in Fig. 7 is the presence of a large amount of aerosol mass in 1991 in the lowermost stratosphere, i.e. below approximately 60 hPa, which is not consistent with SAGE. Potentially the SAGE II-derived data can be still influenced by the known problems in observing the lower stratosphere, which became opaque for limb-occultation instruments in 1991 (Russell et al., 1996). This is partly confirmed by comparison of SAGE II-derived data with HIRS and AVHRR in previous sections. However, recently Revell et al. (2017) analysed the stratospheric warming after Pinatubo using SOCOLvs3, which has the same dynamical and chemical cores as SOCOL-AER, but used prescribed aerosols from the SAGE-4 λ and SAGE-3 λ composites. They found that model simulations driven by SAGE-3 λ aerosols are much closer to temperature reanalyses than simulations driven by SAGE-4 λ , which also has more aerosol mass present in the lowermost tropical stratosphere.

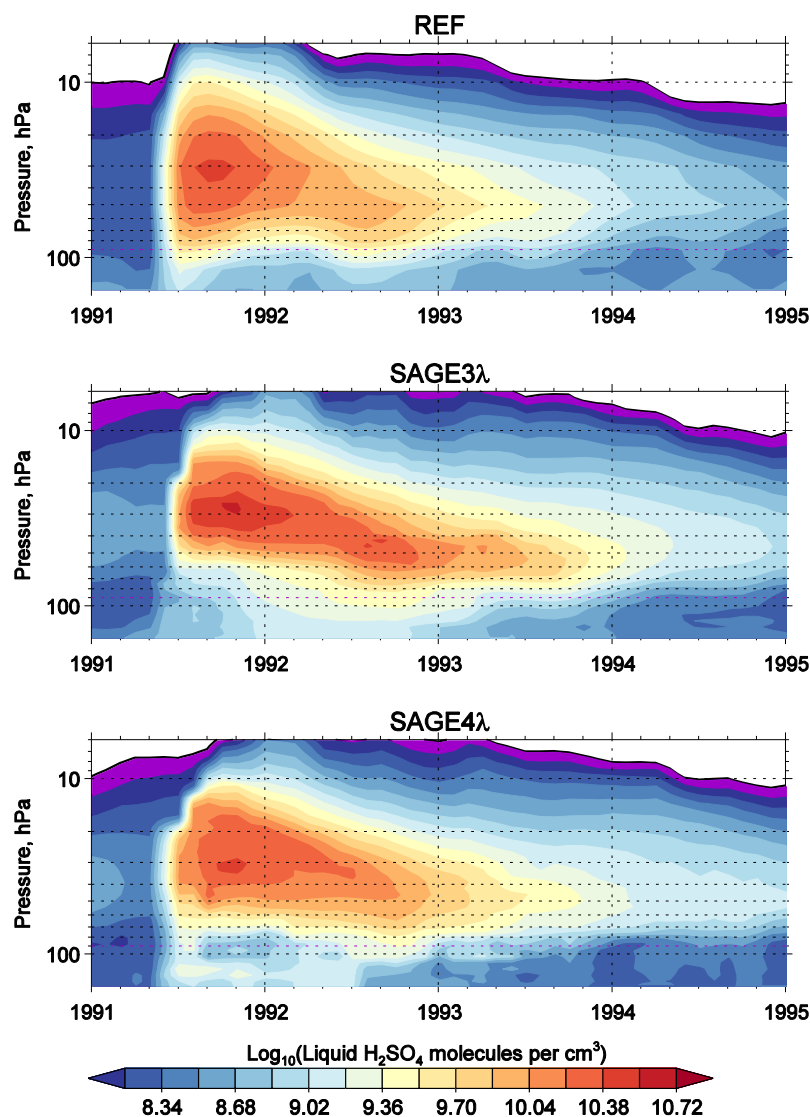


Figure 7. Vertical distribution of liquid H_2SO_4 concentration averaged over the tropics (20°S – 20°N).

We added results of both experiments from Revell et al. (2017) to our Fig. 6 (dashed and dotted blue curves). Analysis
5 of late 1991 reveals that model results driven by SAGE-3 λ are also biased compared to reanalysis temperature but to the
opposite direction than REF. Purely radiatively, this fact suggests that the sharp cut of SAGE-3 λ aerosol cloud below 60 hPa
in late 1991 is not realistic and there should be something in between the REF and SAGE-derived data. However the dynamics
is also highly involved in this region, since modification of warming at different levels also causes changes to the tropical
upwelling and therefore adiabatic cooling of higher levels as well as aerosol redistribution causing further changes to local
10 radiative effects. Besides this, the extra-tropical wave-breaking and thus the stratospheric residual circulation is also modified

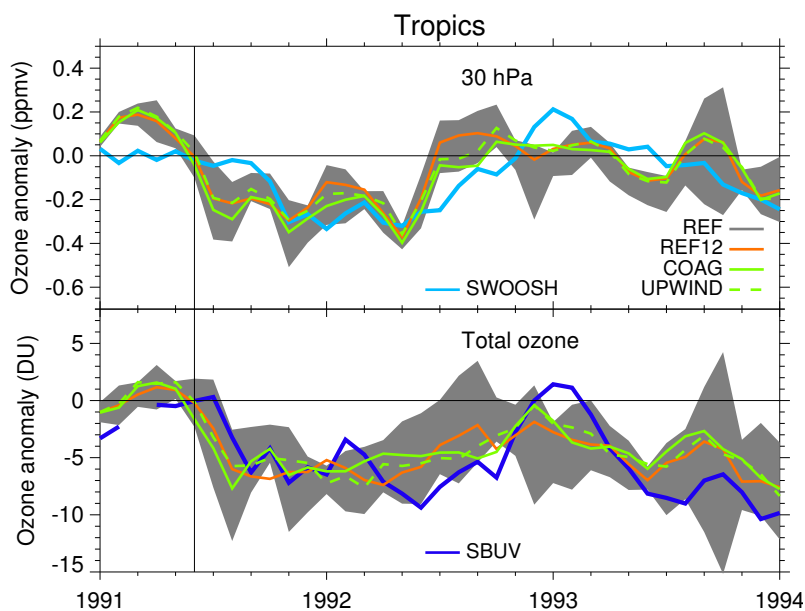


Figure 8. Zonal mean tropical mean (20°S – 20°N) ozone anomalies from SOCOL-AER compared with observations. Upper panel: ozone mixing ratio at 30 hPa. Lower panel: total ozone column. Observational data sets SWOOSH and SBUVv8.6 are denoted by light and dark blue lines, respectively. Anomalies are computed by subtracting the annual cycle. Grey shaded area: $2\text{-}\sigma$ ensemble spread of the REF experiment. All other experiments are shown as ensemble means.

with further consequences for the tropics (e.g. Toohy et al., 2014). Comparison of REF and SAGE results in Figs. 6 and 7 for period after 1991 also suggests that relation of the vertical distribution of aerosol mass and the resulting warming is nonlinear and needs further detailed investigation separating dynamical and radiative effects.

3.4 Ozone response

The response of ozone to major volcanic eruptions is subject to the plethora of dynamical and radiative stratospheric feedbacks including changes in heterogeneous chemistry. (Muthers et al., 2015) showed that even a sign of the total ozone response after a volcanic eruption depends on the background halogen loading of the stratosphere. Volcanic eruptions can in principle also contribute to the stratospheric chlorine which further affects ozone, but there was no significant increase in stratospheric chlorine observed after Pinatubo (Webster et al., 1998). Figure 8 compares monthly mean tropical ozone from SOCOL-AER simulations with the ozone mixing ratio at 30 hPa from the merged satellite composite SWOOSH (Stratospheric Water and Ozone Satellite Homogenized data set, Davis et al., 2016) as well as with the total ozone column from the combined record SBUV (Merged Ozone Data Set version 8.6, McPeters et al., 2013). We focused on tropics since ozone response most pronounced here compared to other regions (e.g. Rozanov et al., 2002). SOCOL-AER captures the maximum ozone loss seen in observations well (around -0.3 ppmv and -7 DU), but leads to slightly premature ozone recovery in 1992. There are small



differences among model scenarios but all of them generally fit the ensemble spread of the reference experiment and have the same issue compared to independent observational time series SWOOSH and SBUV.

4 Conclusions and discussion

15 We have simulated the temporal and spatial development of stratospheric aerosols following the 1991 Pinatubo eruption, as well as temperature and ozone responses, using SOCOL-AER, a free-running 3-D global chemistry-climate model coupled with a particle-size resolving aerosol module. The simulations explore the role of the QBO, aerosol radiative heating, sedimentation scheme and coagulation efficiency in the evolution of the stratospheric aerosol after Pinatubo.

The results show that QBO and interactive aerosol radiative heating play a significant role in maintaining the tropical stratospheric aerosol reservoir over the whole course of the volcanic aerosol cloud evolution. Furthermore, the results suggest that an accurate sedimentation scheme helps to significantly improve the model's ability to reproduce stratospheric aerosol. Numerically diffusive methods, such as a simple upwind method, must be avoided in modeling studies of large volcanic eruptions to prevent artificially fast spreading of particles to high and low altitudes. A more sophisticated coagulation scheme is capable of improving the comparisons with in situ particle size measurements as well as with satellite-borne extinction ratios, which are a proxy for particle sizes. On the other hand, the improved coagulation scheme leads to too rapid sedimentation and loss of stratospheric aerosol mass, which become noticeable in the model about one year after the eruption.

There is significant uncertainty among the observational data of different aerosol parameters. Observations differ by up to $\pm 15\%$ in the global aerosol burden, $\pm 30\%$ in aerosol optical depth and spatiotemporal aerosol distribution in the two years following the eruption, $\pm 40\%$ in the effective particle radii, $\pm 15\%$ in the lower stratospheric temperature anomalies. This renders the exact determination of the required emitted sulfur amount difficult. Thus, the vertically integrated tropical mass simulated by the reference experiment in 1991 (Fig. 1b) is in good agreement with HIRS, but later experiences faster decay that is not consistent with HIRS and SAGE-3 λ but closer to SAGE-4 λ . Considering this fact and relying on SAGE-3 λ after 1991, we can assume that our 14 Tg estimate of initial emission was still sufficient for our model, but the vertical distribution of resulting aerosols could be incorrectly shifted to the lowermost levels. This fact could be responsible for the main modelling deficiency found, namely the 1-2 K larger warming that is inconsistent with temperature reanalyses. It could also explain the integrated modelled burden difference to SAGE-3 λ since 1992 (Fig. 1), as the mass located at lower levels also sediments faster to the troposphere, despite increased buoyancy produced by additional warming. However, if not relying on SAGE-3 λ , our model reveals a very good agreement with AVHRR instrument in terms of AOD in the visible part of the spectrum (Figs. 4 and 5). The experiment with the reduced emission revealed much better representation of the post-eruption stratospheric warming, but at the same time less optimal agreement with observations of other parameters.

There is a rising interest of the climate community to the global models with interactive aerosol microphysics. It is caused partly by the topic of climate geoengineering, namely a compensation of the global warming by artificial emissions of SO₂ (e.g. MacMartin et al., 2016), as well as by the unclear role of major and smaller volcanoes in the future climate (e.g. Bethke et al., 2017). Considering other studies modeling Pinatubo, our simulations corroborate the results of Kleinschmitt et al. (2017)



who also used a sectional model (LDMZ-S3A) and the same emission rate of 14 Tg of SO₂. Their results also revealed overestimation of the stratospheric warming, however they attributed it to the fact that aerosol composition is prescribed during calculation of aerosol optical properties in LDMZ-S3A (Christoph Kleinschmitt, private communication, 2017), which is not the case for SOCOL-AER. The reasons for this overestimation in our case are to be investigated, as SOCOL-AER still undergoes further development. The recent Tambora model intercomparison study by Marshall et al. (2017) demonstrated that SOCOL-AER has substantial problems in representing the absolute values of sulfate deposition to polar regions, due to a simplified tropospheric deposition scheme, but also that SOCOL-AER has the closest agreement with ice-core observations in terms of timing of start and end of volcanic increase in deposition, which is defined by stratospheric aerosol lifetime. A model intercomparison study for Pinatubo is planned within the framework of the Stratospheric Sulfur and Its Role in Climate activity (SSiRC, <http://www.sparc-ssirc.org/>), but, as was also shown here, aerosol observational uncertainty concerning the eruption of Mt. Pinatubo is high and will complicate the derivation of exact conclusions for certain processes and models. Another strong eruption similar to Pinatubo could significantly improve our understanding of the underlying microphysical and transport processes, given recent advances in measuring techniques (Kremser et al., 2016).

5 Code and data availability

SOCOL-AER model code and simulation results presented in this study can be requested by contacting the corresponding author.

Author contributions. JXS and TS performed the simulations, visualized the data, and wrote most of the article. All authors are responsible for code development and discussion of results.

Competing interests. The authors declare that they have no conflict of interest.

Acknowledgements. This work was supported by the Swiss National Science Foundation under the grant 200021-130478(IASSA). ER and TS acknowledge support from the Swiss National Science Foundation under grant 200021-169241 (VEC). AF acknowledges support from the ETH Grant ETH-39 15-2. We thank Michael Mills for discussion of AVHRR data and Christoph Kleinschmitt for discussion about LDMZ-S3A results and for providing the effective radius observational time series.



References

- Aquila, V., Oman, L. D., Stolarski, R. S., Colarco, P. R., and Newman, P. A.: Dispersion of the volcanic sulfate cloud from a Mount Pinatubo-like eruption, *Journal of Geophysical Research: Atmospheres*, 117, n/a–n/a, doi:10.1029/2011JD016968, <http://onlinelibrary.wiley.com/doi/10.1029/2011JD016968/abstract>, 2012.
- 5 Arfeuille, F., Luo, B. P., Heckendorn, P., Weisenstein, D., Sheng, J. X., Rozanov, E., Schraner, M., Brönnimann, S., Thomason, L. W., and Peter, T.: Modeling the stratospheric warming following the Mt. Pinatubo eruption: uncertainties in aerosol extinctions, *Atmos. Chem. Phys.*, 13, 11 221–11 234, doi:10.5194/acp-13-11221-2013, <http://www.atmos-chem-phys.net/13/11221/2013/>, 2013.
- Baran, A. J. and Foot, J. S.: New application of the operational sounder HIRS in determining a climatology of sulphuric acid aerosol from the Pinatubo eruption, *Journal of Geophysical Research: Atmospheres*, 99, 25 673–25 679, doi:10.1029/94JD02044, <http://onlinelibrary.wiley.com/doi/10.1029/94JD02044/abstract>, 1994.
- 10 Bekki, S.: Oxidation of volcanic SO₂: A sink for stratospheric OH and H₂O, *Geophysical Research Letters*, 22, 913–916, doi:10.1029/95GL00534, 1995.
- Benduhn, F. and Lawrence, M. G.: An investigation of the role of sedimentation for stratospheric solar radiation management, *Journal of Geophysical Research: Atmospheres*, 118, 7905–7921, doi:10.1002/jgrd.50622, <http://onlinelibrary.wiley.com/doi/10.1002/jgrd.50622/abstract>, 2013.
- 15 Bethke, I., Outten, S., Otterå, O. H., Hawkins, E., Wagner, S., Sigl, M., and Thorne, P.: Potential volcanic impacts on future climate variability, *Nature Climate Change*, 7, 799–805, doi:10.1038/nclimate3394, 2017.
- CCMVal: Report on the Evaluation of Chemistry-Climate Models, edited by: Eyring, V., Shepherd, TG, and Waugh, DW, Tech. rep., SPARC Report No. 5, 2010.
- 20 Davis, S. M., Rosenlof, K. H., Hassler, B., Hurst, D. F., Read, W. G., Vömel, H., Selkirk, H., Fujiwara, M., and Damadeo, R.: The Stratospheric Water and Ozone Satellite Homogenized (SWOOSH) database: a long-term database for climate studies, *Earth System Science Data*, 8, 461–490, doi:10.5194/essd-8-461-2016, 2016.
- Deshler, T.: A review of global stratospheric aerosol: Measurements, importance, life cycle, and local stratospheric aerosol, *Atmospheric Research*, 90, 223–232, doi:10.1016/j.atmosres.2008.03.016, <http://www.sciencedirect.com/science/article/pii/S0169809508000598>, 2008.
- 25 Deshler, T., Hervig, M. E., Hofmann, D. J., Rosen, J. M., and Liley, J. B.: Thirty years of in situ stratospheric aerosol size distribution measurements from Laramie, Wyoming (41°N), using balloon-borne instruments, *Journal of Geophysical Research: Atmospheres*, 108, n/a–n/a, doi:10.1029/2002JD002514, <http://onlinelibrary.wiley.com/doi/10.1029/2002JD002514/abstract>, 2003.
- Dhomse, S. S., Emmerson, K. M., Mann, G. W., Bellouin, N., Carslaw, K. S., Chipperfield, M. P., Hommel, R., Abraham, N. L., Telford, P., Braesicke, P., Dalvi, M., Johnson, C. E., O'Connor, F., Morgenstern, O., Pyle, J. A., Deshler, T., Zawodny, J. M., and Thomason, L. W.: Aerosol microphysics simulations of the Mt. Pinatubo eruption with the UM-UKCA composition-climate model, *Atmospheric Chemistry & Physics*, 14, 11 221–11 246, doi:10.5194/acp-14-11221-2014, 2014.
- 30 Dutton, E. G. and Christy, J. R.: Solar radiative forcing at selected locations and evidence for global lower tropospheric cooling following the eruptions of El Chichón and Pinatubo, *Geophysical Research Letters*, 19, 2313–2316, doi:10.1029/92GL02495, <http://onlinelibrary.wiley.com/doi/10.1029/92GL02495/abstract>, 1992.
- 35 English, J. M., Toon, O. B., Mills, M. J., and Yu, F.: Microphysical simulations of new particle formation in the upper troposphere and lower stratosphere, *Atmos. Chem. Phys.*, 11, 9303–9322, doi:10.5194/acp-11-9303-2011, <http://www.atmos-chem-phys.net/11/9303/2011/>, 2011.



- English, J. M., Toon, O. B., and Mills, M. J.: Microphysical simulations of large volcanic eruptions: Pinatubo and Toba, *Journal of Geophysical Research: Atmospheres*, 118, 1880–1895, doi:10.1002/jgrd.50196, <http://onlinelibrary.wiley.com/doi/10.1002/jgrd.50196/abstract>, 2013.
- 5 Eyring, V., Butchart, N., Waugh, D. W., Akiyoshi, H., Austin, J., Bekki, S., Bodeker, G. E., Boville, B. A., Brühl, C., Chipperfield, M. P., Cordero, E., Dameris, M., Deushi, M., Fioletov, V. E., Frith, S. M., Garcia, R. R., Gettelman, A., Giorgetta, M. A., Grewe, V., Jourdain, L., Kinnison, D. E., Mancini, E., Manzini, E., Marchand, M., Marsh, D. R., Nagashima, T., Newman, P. A., Nielsen, J. E., Pawson, S., Pitari, G., Plummer, D. A., Rozanov, E., Schraner, M., Shepherd, T. G., Shibata, K., Stolarski, R. S., Struthers, H., Tian, W., and Yoshiki, M.: Assessment of temperature, trace species, and ozone in chemistry-climate model simulations of the recent past, *Journal of Geophysical Research: Atmospheres*, 111, D22 308, doi:10.1029/2006JD007327, <http://onlinelibrary.wiley.com/doi/10.1029/2006JD007327/abstract>, 10 2006.
- Eyring, V., Bony, S., Meehl, G. A., Senior, C. A., Stevens, B., Stouffer, R. J., and Taylor, K. E.: Overview of the Coupled Model Intercomparison Project Phase 6 (CMIP6) experimental design and organization, *Geoscientific Model Development*, 9, 1937–1958, doi:10.5194/gmd-9-1937-2016, 2016.
- 15 Graf, H.-F., Li, Q., and Giorgetta, M. A.: Volcanic effects on climate: revisiting the mechanisms, *Atmos. Chem. Phys.*, 7, 4503–4511, doi:10.5194/acp-7-4503-2007, <http://www.atmos-chem-phys.net/7/4503/2007/>, 2007.
- Guo, S., Bluth, G. J. S., Rose, W. I., Watson, I. M., and Prata, A. J.: Re-evaluation of SO₂ release of the 15 June 1991 Pinatubo eruption using ultraviolet and infrared satellite sensors, *Geochemistry, Geophysics, Geosystems*, 5, n/a–n/a, doi:10.1029/2003GC000654, <http://onlinelibrary.wiley.com/doi/10.1029/2003GC000654/abstract>, 2004.
- 20 Kleinschmitt, C., Boucher, O., Bekki, S., Lott, F., and Platt, U.: The Sectional Stratospheric Sulfate Aerosol module (S3A-v1) within the LMDZ general circulation model: description and evaluation against stratospheric aerosol observations, *Geoscientific Model Development*, 10, 3359–3378, doi:10.5194/gmd-10-3359-2017, 2017.
- Kodera, K.: Influence of volcanic eruptions on the troposphere through stratospheric dynamical processes in the northern hemisphere winter, *Journal of Geophysical Research: Atmospheres*, 99, 1273–1282, doi:10.1029/93JD02731, <http://onlinelibrary.wiley.com/doi/10.1029/93JD02731/abstract>, 1994.
- 25 Kremser, S., Thomason, L. W., von Hobe, M., Hermann, M., Deshler, T., Timmreck, C., Toohey, M., Stenke, A., Schwarz, J. P., Weigel, R., Fueglistaler, S., Prata, F. J., Vernier, J.-P., Schlager, H., Barnes, J. E., Antuña-Marrero, J.-C., Fairlie, D., Palm, M., Mahieu, E., Notholt, J., Rex, M., Bingen, C., Vanhellemont, F., Bourassa, A., Plane, J. M. C., Klocke, D., Carn, S. A., Clarisse, L., Trickl, T., Neely, R., James, A. D., Rieger, L., Wilson, J. C., and Meland, B.: Stratospheric aerosol: Observations, processes, and impact on climate, *Reviews of Geophysics*, 54, 278–335, doi:10.1002/2015RG000511, 2016.
- 30 Labitzke, K. and McCormick, M. P.: Stratospheric temperature increases due to Pinatubo aerosols, *Geophysical Research Letters*, 19, 207–210, doi:10.1029/91GL02940, <http://onlinelibrary.wiley.com/doi/10.1029/91GL02940/abstract>, 1992.
- Lacis, A., Hansen, J., and Sato, M.: Climate forcing by stratospheric aerosols, *Geophysical Research Letters*, 19, 1607–1610, doi:10.1029/92GL01620, 1992.
- Lanzante, J. R. and Free, M.: Comparison of Radiosonde and GCM Vertical Temperature Trend Profiles: Effects of Dataset Choice and Data Homogenization*, *Journal of Climate*, 21, 5417–5435, doi:10.1175/2008JCLI2287.1, <http://journals.ametsoc.org/doi/abs/10.1175/2008JCLI2287.1>, 2008.
- 35 Liu, F., Chai, J., Wang, B., Liu, J., Zhang, X., and Wang, Z.: Global monsoon precipitation responses to large volcanic eruptions, *Scientific Reports*, 6, 24331, doi:10.1038/srep24331, 2016.



- MacMartin, D. G., Kravitz, B., Long, J. C. S., and Rasch, P. J.: Geoengineering with stratospheric aerosols: What do we not know after a decade of research?, *Earth's Future*, 4, 543–548, doi:10.1002/2016EF000418, <http://dx.doi.org/10.1002/2016EF000418>, 2016EF000418, 2016.
- Marshall, L., Schmidt, A., Toohey, M., Carslaw, K. S., Mann, G. W., Sigl, M., Khodri, M., Timmreck, C., Zanchettin, D., Ball, W., Bekki, S., Brooke, J. S. A., Dhomse, S., Johnson, C., Lamarque, J.-F., LeGrande, A., Mills, M. J., Niemeier, U., Poulain, V., Robock, A., Rozanov, E., Stenke, A., Sukhodolov, T., Tilmes, S., Tsigaridis, K., and Tummon, F.: Multi-model comparison of the volcanic sulfate deposition from the 1815 eruption of Mt. Tambora, *Atmospheric Chemistry and Physics Discussions*, 2017, 1–39, doi:10.5194/acp-2017-729, <https://www.atmos-chem-phys-discuss.net/acp-2017-729/>, 2017.
- McPeters, R. D., Bhartia, P. K., Haffner, D., Labow, G. J., and Flynn, L.: The version 8.6 SBUV ozone data record: An overview, *Journal of Geophysical Research (Atmospheres)*, 118, 8032–8039, doi:10.1002/jgrd.50597, 2013.
- Miles, G. M., Siddans, R., Grainger, R. G., Prata, A. J., Fisher, B., and Krotkov, N.: Retrieval of volcanic SO₂ from HIRS/2 using optimal estimation, *Atmospheric Measurement Techniques*, 10, 2687–2702, doi:10.5194/amt-10-2687-2017, 2017.
- Mills, M. J., Schmidt, A., Easter, R., Solomon, S., Kinnison, D. E., Ghan, S. J., Neely, R. R., Marsh, D. R., Conley, A., Bardeen, C. G., and Gettelman, A.: Global volcanic aerosol properties derived from emissions, 1990–2014, using CESM1(WACCM), *Journal of Geophysical Research (Atmospheres)*, 121, 2332–2348, doi:10.1002/2015JD024290, 2016.
- Mills, M. J., Richter, J. H., Tilmes, S., Kravitz, B., MacMartin, D. G., Glanville, A. A., Tribbia, J. J., Lamarque, J.-F., Vitt, F., Schmidt, A., Gettelman, A., Hannay, C., Bacmeister, J. T., and Kinnison, D. E.: Radiative and Chemical Response to Interactive Stratospheric Sulfate Aerosols in Fully Coupled CESM1(WACCM), *Journal of Geophysical Research: Atmospheres*, pp. n/a–n/a, doi:10.1002/2017JD027006, <http://dx.doi.org/10.1002/2017JD027006>, 2017JD027006, 2017.
- Minnis, P., Harrison, E. F., Stowe, L. L., Gibson, G. G., Denn, F. M., Doelling, D. R., and Smith, W. L.: Radiative Climate Forcing by the Mount Pinatubo Eruption, *Science*, 259, 1411–1415, doi:10.1126/science.259.5100.1411, <http://www.sciencemag.org/content/259/5100/1411>, PMID: 17801273, 1993.
- Muthers, S., Arfeuille, F., Raible, C. C., and Rozanov, E.: The impacts of volcanic aerosol on stratospheric ozone and the Northern Hemisphere polar vortex: separating radiative-dynamical changes from direct effects due to enhanced aerosol heterogeneous chemistry, *Atmospheric Chemistry and Physics*, 15, 11461–11476, doi:10.5194/acp-15-11461-2015, <https://www.atmos-chem-phys.net/15/11461/2015/>, 2015.
- Narsimhan, G. and Ruckenstein, E.: The Brownian coagulation of aerosols over the entire range of Knudsen numbers: Connection between the sticking probability and the interaction forces, *Journal of Colloid and Interface Science*, 104, 344–369, doi:10.1016/0021-9797(85)90044-X, <http://www.sciencedirect.com/science/article/pii/002197978590044X>, 1985.
- Predybaylo, E., Stenchikov, G. L., Wittenberg, A. T., and Zeng, F.: Impacts of a Pinatubo-size volcanic eruption on ENSO, *Journal of Geophysical Research (Atmospheres)*, 122, 925–947, doi:10.1002/2016JD025796, 2017.
- Randel, W. J., Shine, K. P., Austin, J., Barnett, J., Claud, C., Gillett, N. P., Keckhut, P., Langematz, U., Lin, R., Long, C., Mears, C., Miller, A., Nash, J., Seidel, D. J., Thompson, D. W. J., Wu, F., and Yoden, S.: An update of observed stratospheric temperature trends, *Journal of Geophysical Research: Atmospheres*, 114, n/a–n/a, doi:10.1029/2008JD010421, <http://onlinelibrary.wiley.com/doi/10.1029/2008JD010421/abstract>, 2009.
- Revell, L. E., Stenke, A., Luo, B., Kremser, S., Rozanov, E., Sukhodolov, T., and Peter, T.: Impacts of Mt Pinatubo volcanic aerosol on the tropical stratosphere in chemistry-climate model simulations using CCM1 and CMIP6 stratospheric aerosol data, *Atmospheric Chemistry & Physics*, 17, 13139–13150, doi:10.5194/acp-17-13139-2017, 2017.



- Rozanov, E. V., Schlesinger, M. E., Andronova, N. G., Yang, F., Malyshev, S. L., Zubov, V. A., Egorova, T. A., and Li, B.: Climate/chemistry effects of the Pinatubo volcanic eruption simulated by the UIUC stratosphere/troposphere GCM with interactive photochemistry, *Journal of Geophysical Research: Atmospheres*, 107, ACL 12–1–ACL 12–14, doi:10.1029/2001JD000974, <http://dx.doi.org/10.1029/2001JD000974>, 4594, 2002.
- 5 Russell, P. B., Livingston, J. M., Pueschel, R. F., Bauman, J. J., Pollack, J. B., Brooks, S. L., Hamill, P., Thomason, L. W., Stowe, L. L., Deshler, T., Dutton, E. G., and Bergstrom, R. W.: Global to microscale evolution of the Pinatubo volcanic aerosol derived from diverse measurements and analyses, *Journal of Geophysical Research: Atmospheres*, 101, 18 745–18 763, doi:10.1029/96JD01162, <http://onlinelibrary.wiley.com/doi/10.1029/96JD01162/abstract>, 1996.
- Sekiya, T., Sudo, K., and Nagai, T.: Evolution of stratospheric sulfate aerosol from the 1991 Pinatubo eruption: Roles of aerosol microphysical
10 processes, *Journal of Geophysical Research (Atmospheres)*, 121, 2911–2938, doi:10.1002/2015JD024313, 2016.
- Sheng, J.-X., Weisenstein, D. K., Luo, B.-P., Rozanov, E., Arfeuille, F., and Peter, T.: A perturbed parameter model ensemble to investigate Mt. Pinatubo’s 1991 initial sulfur mass emission, *Atmospheric Chemistry & Physics*, 15, 11 501–11 512, doi:10.5194/acp-15-11501-2015, 2015a.
- Sheng, J.-X., Weisenstein, D. K., Luo, B.-P., Rozanov, E., Stenke, A., Anet, J., Bingemer, H., and Peter, T.: Global atmospheric sulfur
15 budget under volcanically quiescent conditions: Aerosol-chemistry-climate model predictions and validation, *J. Geophys. Res. Atmos.*, 120, 2014JD021 985, doi:10.1002/2014JD021985, <http://onlinelibrary.wiley.com/doi/10.1002/2014JD021985/abstract>, 2015b.
- Sigl, M., Winstrup, M., McConnell, J. R., Welten, K. C., Plunkett, G., Ludlow, F., Büntgen, U., Caffee, M., Chellman, N., Dahl-Jensen, D., Fischer, H., Kipfstuhl, S., Kostick, C., Maselli, O. J., Mekhaldi, F., Mulvaney, R., Muscheler, R., Pasteris, D. R., Pilcher, J. R., Salzer, M., Schüpbach, S., Steffensen, J. P., Vinther, B. M., and Woodruff, T. E.: Timing and climate forcing of volcanic eruptions for the past 2,500
20 years, *Nature*, 523, 543–549, doi:10.1038/nature14565, 2015.
- Soden, B. J., Wetherald, R. T., Stenchikov, G. L., and Robock, A.: Global Cooling After the Eruption of Mount Pinatubo: A Test of Climate Feedback by Water Vapor, *Science*, 296, 727–730, doi:10.1126/science.296.5568.727, 2002.
- Solomon, S.: Stratospheric ozone depletion: A review of concepts and history, *Reviews of Geophysics*, 37, 275–316, doi:10.1029/1999RG900008, <http://www.agu.org/pubs/crossref/1999/1999RG900008.shtml>, 1999.
- 25 Stenke, A., Schraner, M., Rozanov, E., Egorova, T., Luo, B., and Peter, T.: The SOCOL version 3.0 chemistry-climate model: description, evaluation, and implications from an advanced transport algorithm, *Geoscientific Model Development*, 6, 1407–1427, doi:10.5194/gmd-6-1407-2013, 2013.
- Swingedouw, D., Mignot, J., Ortega, P., Khodri, M., Menegoz, M., Cassou, C., and Hanquiez, V.: Impact of explosive volcanic eruptions on the main climate variability modes, *Global and Planetary Change*, 150, 24–45, doi:10.1016/j.gloplacha.2017.01.006, 2017.
- 30 Telford, P., Braesicke, P., Morgenstern, O., and Pyle, J.: Reassessment of causes of ozone column variability following the eruption of Mount Pinatubo using a nudged CCM, *Atmospheric Chemistry & Physics Discussions*, 9, 5423–5446, 2009.
- Thompson, D. W. J., Wallace, J. M., Jones, P. D., and Kennedy, J. J.: Identifying Signatures of Natural Climate Variability in Time Series of Global-Mean Surface Temperature: Methodology and Insights, *Journal of Climate*, 22, 6120, doi:10.1175/2009JCLI3089.1, 2009.
- Timmreck, C., Graf, H.-F., and Feichter, J.: Simulation of Mt. Pinatubo Volcanic Aerosol with the Hamburg Climate Model ECHAM4,
35 Theoretical and Applied Climatology, 62, 85–108, doi:10.1007/s007040050076, <http://link.springer.com/article/10.1007/s007040050076>, 1999a.



- Timmreck, C., Graf, H.-F., and Kirchner, I.: A one and half year interactive MA/ECHAM4 simulation of Mount Pinatubo Aerosol, *Journal of Geophysical Research: Atmospheres*, 104, 9337–9359, doi:10.1029/1999JD900088, <http://onlinelibrary.wiley.com/doi/10.1029/1999JD900088/abstract>, 1999b.
- Timmreck, C., Pohlmann, H., Illing, S., and Kadow, C.: The impact of stratospheric volcanic aerosol on decadal-scale climate predictions, *Geophysical Research Letters*, 43, 834–842, doi:10.1002/2015GL067431, 2016.
- 5 Toohey, M. and Sigl, M.: Volcanic stratospheric sulfur injections and aerosol optical depth from 500 BCE to 1900 CE, *Earth System Science Data*, 9, 809–831, doi:10.5194/essd-9-809-2017, <https://www.earth-syst-sci-data.net/9/809/2017/>, 2017.
- Toohey, M., Krüger, K., Bittner, M., Timmreck, C., and Schmidt, H.: The impact of volcanic aerosol on the Northern Hemisphere stratospheric polar vortex: mechanisms and sensitivity to forcing structure, *Atmospheric Chemistry and Physics*, 14, 13 063–13 079, doi:10.5194/acp-14-13063-2014, <https://www.atmos-chem-phys.net/14/13063/2014/>, 2014.
- 10 Trepte, C. R. and Hitchman, M. H.: Tropical stratospheric circulation deduced from satellite aerosol data, *Nature*, 355, 626–628, doi:10.1038/355626a0, <http://www.nature.com/nature/journal/v355/n6361/abs/355626a0.html>, 1992.
- Trepte, C. R., Veiga, R. E., and McCormick, M. P.: The poleward dispersal of Mount Pinatubo volcanic aerosol, *Journal of Geophysical Research: Atmospheres*, 98, 18 563–18 573, doi:10.1029/93JD01362, <http://onlinelibrary.wiley.com/doi/10.1029/93JD01362/abstract>, 1993.
- 15 Walcek, C. J.: Minor flux adjustment near mixing ratio extremes for simplified yet highly accurate monotonic calculation of tracer advection, *Journal of Geophysical Research: Atmospheres*, 105, 9335–9348, doi:10.1029/1999JD901142, <http://onlinelibrary.wiley.com/doi/10.1029/1999JD901142/abstract>, 2000.
- Webster, C. R., May, R. D., Michelsen, H. A., Scott, D. C., Wilson, J. C., Jonsson, H. H., Brock, C. A., Dye, J. E., Baumgardner, D., Stimpfle, R. M., Koplow, J. P., Margitan, J. J., Proffitt, M. H., Jaegl?, L., Herman, R. L., Hu, H., Flesch, G. J., and Loewenstein, M.: Evolution of HCL concentrations in the lower stratosphere from 1991 to 1996 following the eruption of Mt. Pinatubo, *Geophysical Research Letters*, 25, 995–998, doi:10.1029/98GL00548, <http://dx.doi.org/10.1029/98GL00548>, 1998.
- 20 Weisenstein, D. K., Penner, J. E., Herzog, M., and Liu, X.: Global 2-D intercomparison of sectional and modal aerosol modules, *Atmos. Chem. Phys.*, 7, 2339–2355, doi:10.5194/acp-7-2339-2007, <http://www.atmos-chem-phys.net/7/2339/2007/>, 2007.
- Zanchettin, D., Khodri, M., Timmreck, C., Toohey, M., Schmidt, A., Gerber, E. P., Hegerl, G., Robock, A., Pausata, F. S. R., Ball, W. T., Bauer, S. E., Bekki, S., Dhomse, S. S., LeGrande, A. N., Mann, G. W., Marshall, L., Mills, M., Marchand, M., Niemeier, U., Poulain, V., Rozanov, E., Rubino, A., Stenke, A., Tsigaridis, K., and Tummon, F.: The Model Intercomparison Project on the climatic response to Volcanic forcing (VolMIP): experimental design and forcing input data for CMIP6, *Geoscientific Model Development*, 9, 2701–2719, doi:10.5194/gmd-9-2701-2016, <https://www.geosci-model-dev.net/9/2701/2016/>, 2016.
- 25 Zhao, T. X.-P., Chan, P. K., and Heidinger, A. K.: A global survey of the effect of cloud contamination on the aerosol optical thickness and its long-term trend derived from operational AVHRR satellite observations, *Journal of Geophysical Research (Atmospheres)*, 118, 2849–2857, doi:10.1002/jgrd.50278, 2013.
- 30